analytical chemistry

Technical Note

Cite This: *Anal. Chem.* 2019, 91, 3233−3238

pubs.acs.org/ac

Luminescence Lifetime Imaging of Chemical Sensors—A Comparison between Time-Domain and Frequency-Domain Based Camera Systems

Klaus Koren,[*,§,†] Maria Moßhammer,[§,∥] Vincent V. Scholz,[◊] Sergey M. Borisov,[#] Gerhard Holst,[○] and Michael Kühl[*,¥,∥]

[†]Aarhus University Centre for Water Technology, Section for Microbiology, Department of Bioscience, Aarhus University, Ny Munkegade, DK-8000 Aarhus C, Denmark

[∥]Marine Biological Section, Department of Biology, University of Copenhagen, Strandpromenaden 5, DK-3000 Helsingør, Denmark

[◊]Center for Electromicrobiology, Aarhus University, DK-8000 Aarhus, Denmark

[#]Institute of Analytical Chemistry and Food Chemistry, Graz University of Technology, Stremayrgasse 9, AT-8010 Graz, Austria

[○]PCO AG, Donaupark 11, 93309 Kelheim, Germany

[¥]Climate Change Cluster, University of Technology Sydney, Ultimo, NSW 2007, Australia

Supporting Information

ABSTRACT: Luminescence lifetime based imaging is still the most reliable method for generating chemical images using chemical sensor technology. However, only few commercial systems are available that enable imaging lifetimes within the relevant nanosecond to microsecond range. In this technical note we compare the performance of an older time-domain (TD) based camera system with a frequency-domain (FD) based camera system regarding their measuring characteristics and applicability for O_2 and pH imaging in environmental samples and with different indicator dye systems emitting in the visible and near-infrared part of the spectrum. We conclude that the newly introduced FD imaging system delivers comparable if not better results than its predecessor, now enabling robust and simple chemical imaging based on FD luminescence lifetime measurements.

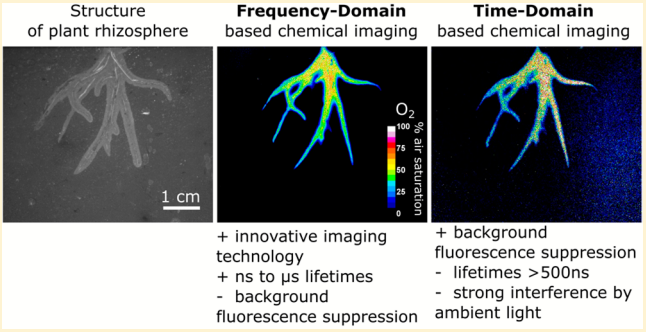

Chemical imaging using luminescent optical sensors is a unique method to visualize the concentration and dynamics of analytes in 2D and 3D.[1] Over the years sensor materials in the form of planar sensor foils (planar optodes) as well as sensor particles were developed for a multitude of analytes[2] such as O_2,[3,4] pH,[5] H_2S,[6] CO_2,[7] or NH_3[8] allowing reversible, real-time concentration measurements.[9] The enormous potential of this method has inspired multiple developments in the field, ranging from multiparameter sensors[10,11] to easy-to-use imaging set-ups.[12] In recent years, ratiometric luminescence intensity imaging has gained importance due to its low cost and easily accessible equipment.[12−15] Nevertheless, luminescence lifetime-based imaging of chemical sensors, especially phosphorescent indicators, is still widely used and considered the most reliable method among experts in the field.[16,17] Lifetime-based chemical imaging was developed >20 years ago and quickly outcompeted simple luminescence intensity-based imaging methods.[18−20] In particular, the accessibility of fast gateable charge coupled devices (CCDs) with on-chip charge accumulation enabled the development of time-domain (TD) luminescence lifetime camera systems for rapid lifetime determination (RLD) in phosphorescence-based chemical imaging. This technique established itself in the 1990s, when PCO released the Sensicam Sensimod, a commercial device capable of RLD-based phosphorescence imaging. Several research groups acquired this camera system and developed sensors and methods[21] suitable particularly for this camera. Unfortunately, CCDs needed for the Sensicam are no longer produced, but these lifetime imaging systems are still used extensively.[22−29]

In this technical note we discuss the potential of a newly developed alternative to the Sensimod camera system. Based on a modulatable scientific complementary metal-oxide semiconductor (sCMOS) sensor, PCO developed a frequency-domain (FD) luminescence lifetime imaging camera, the so-called pco.flim.[30] While this system has found first applications in fluorescence lifetime imaging, its potential for

Received: December 20, 2018
Accepted: February 13, 2019
Published: February 13, 2019

DOI: 10.1021/acs.analchem.8b05869
Anal. Chem. 2019, 91, 3233−3238

chemical imaging using phosphorescent indicators has not yet been evaluated thoroughly. Here we compare the two camera systems in terms of potential for chemical imaging with planar optodes based on phosphorescent indicators with lifetimes in the μs range. In particular, we use O_2 and pH sensors as a test system and evaluate the possibility of performing dual lifetime referencing (DLR).[31]

EXPERIMENTAL SECTION

Imaging Setup. Optodes (Supporting Note 3) were fixed inside a 10 L aquarium or rhizo-sandwich (Supporting Note 4) and imaged with the camera system positioned perpendicular to the transparent aquarium wall. Both cameras were equipped with the same Zeiss Makro Planar 2/100 objective, using a Hama C for Nikon adaptor. The aperture was kept at 2.8 throughout all experiments, and the objective was mounted with either a Schott RG610 (for O_2 imaging) or RG9 (for pH imaging) emission filter.

Time-Domain Camera System. This system, described in detail by Holst et al.,[18] is built around the thermoelectrically cooled, fast gateable, CCD camera Sensicam Sensimod (PCO AG, Germany). Pulsed LEDs (Photonics Research Systems Ltd., UK) were used as an excitation source. For O_2 imaging, two different LEDs (460 nm, 520 nm) were used. A custom-made trigger box, described in other publications,[32] controlled the modulation of the LED array, the shutter and image capturing. The camera and the trigger unit are controlled by the software Look@Molli v1.82a (Holst and Grunwald[19]). The data (dark image, window 1 and 2) were saved in tiff format and analyzed according to a standard procedure (Supporting Note 3).

Frequency-Domain (FD) Camera System. A modulated sCMOS camera (pco.flim, PCO AG, Germany), functions as a trigger and sends the modulation frequency to the light source in this case a LEDHUB (Omicron Laserage, Germany) connected to the TTL output of the camera via an included adaptor. A 1 m liquid light guide delivered the emission of one of three LEDs (460, 528, and 625 nm) in the LEDHUB to the sample. Blue light was used to excite foils containing Macrolex Yellow (MY), green for foils containing only PtTFPP, and red for the pH-sensitive foil. The Omicron LEDHUB control software was used to adjust the LED intensity and to enable the camera trigger. Other imaging-related parameters were set using the Nikon NIS Elements Advanced Research software, which was used for system control, data acquisition, and image processing. The modulation frequency was set to 5 kHz. Before imaging of a sample, a lifetime reference image was recorded. This can either be done by imaging a sample with known lifetime (ns or μs) or by using the reflected light of the LED (remove emission filter or use other LED) as a reference. When using reflected light, the known "lifetime" is very short (at least 1000 times shorter) in comparison to the phosphorescence lifetime of the indicator, thus in practice the reference lifetime can be set to 0 μs. The software enables export of phase shift, modulation, modulation lifetime, and phase lifetime as well as all the intensity images. In this study phase shift and phase lifetime images were exported and analyzed (Supporting Note 3).

RESULTS AND DISCUSSION

Lifetime-Based Chemical Imaging—Time-Domain versus Frequency-Domain. Chemical imaging with sensors enables the visualization of chemical species in 2D and 3D. Camera systems are essential for such kind of analysis. In comparison to luminescence intensity-based imaging approaches, luminescence lifetime-based imaging has distinct advantages including self-referencing, less susceptibility to bleaching or leaching related artifacts, and less interfering background luminescence. Luminescence lifetimes can be determined either via time-domain or frequency-domain mode (Figure S1).[2] In the TD, the emission is followed over time, whereas in FD the phase shift of the emission is followed relative to the modulated excitation.

Time-domain systems support various sensing modes, such as rapid lifetime determination (RLD, Figure S1A) or dual lifetime referencing (DLR, Figure S1B). Luminescence lifetimes are acquired according to eq 1 for RLD based imaging.

$$\tau = \frac{t_2 - t_1}{\ln \frac{A_1}{A_2}} \tag{1}$$

In this imaging mode a square shaped excitation pulse is used to excite the luminophore. After excitation, images are recorded in two time windows of the same length at certain time points (t_1 and t_2) during the decay phase of the luminophore, in order to reconstruct the exponential decay of the luminescence signal. Due to the formed ratio of the two intensity images (A_1/A_2) the system is not affected by e.g. inhomogeneous sensor distribution in foils, reflections, photobleaching of the indicator dye, drifting sensitivity of the photodetector, or fluctuations in the excitation source.[33] DLR relies on the addition of a reference dye of longer lifetime along with the luminescent indicator.[33,34] Both dyes are excitable at the same wavelength and show overlapping emission spectra.

FD measurements use continuous, sinusoidally modulated excitation instead of a pulsed excitation.[33,35] The resulting luminescence emission of the indicator dye is sinusoidally modulated following the excitation frequency but is phase-shifted by an angle, φ, depending on the luminescence lifetime of the indicator dye[33] (Figure S1C). The FD lifetime camera system reconstructs the sinusoidal signal (see the SI for details), from which φ and the modulation index (m) can be determined using the excitation and emission amplitudes (a_{em} and a_{exc}) divided by their constant components b_{em} and b_{exc} (eq 2; Figure S1C). This is then used together with a separate reference measurement to determine lifetimes (eq 3), where f_{mod} is the modulation frequency. In the FD camera system a special CMOS image sensor is used which incorporates a special so-called "charge-swing" in each pixel, which allows directing the charge carriers in two different taps for collection at a very high modulation frequency (Figure S5). This builds the basis of the FD lifetime determination used in the pco.flim.

$$m = \frac{a_{em}/b_{em}}{a_{exc}/b_{exc}} \tag{2}$$

$$\tau = \frac{\tan(\varphi)}{2\pi f_{mod}} \tag{3}$$

The characteristics of both camera systems are compared in Table 1, while a more detailed description of their imaging acquisition principles can be found in Supporting Note 1. Since both types of approaches measure luminescence lifetime distributions, the TD and the FD methods are in principle

DOI: 10.1021/acs.analchem.8b05869
Anal. Chem. 2019, 91, 3233−3238

Table 1. Characteristics of the Two Camera Systems for TD and FD Luminescence Lifetime Imaging[18,35]

	Sensicam Sensimod	pco.flim
measurement mode	time-domain	frequency-domain
image sensor	CCD	CMOS
resolution	1280 × 1024 pixel (depending on binning)	1008 × 1008 pixel
pixel size	6.7 μm × 6.7 μm	5.6 μm × 5.6 μm
frame rate	8 frames/s	45 double frames/s
quantum efficiency	42% @ 480 nm	39% @ 510 nm
image sensor temperature	−12 °C	+5 °C
readout noise	8 e^-	48 e^-
Fulwell capacity	25000 e^-	53000 e^-
dynamic range	1:3125	1:1104
A/D converter	12 bit	14 bit
power consumption	19 W	40 W
shutter speed	$t_{on/off}$ = 500 ns; maximum frequency = 1 MHz	
modulation frequency range "out"		5 kHz−40 MHz
modulation frequency range "in"	1−350 Hz	500 kHz−40 MHz
modulation signal shape	square wave	sinusoidal/square wave
lifetimes	500 ns−1 s	100 ps−100 μs
exposure times	250 ns−450 ms	1 ms−2 s
ambient temperature	0−40 °C	5−40 °C

yielding equivalent results, but differences can arise from the technical layout of the available image sensors.

CCD image sensors are inherently slow due to their serial readout principle but usually have low dark currents allowing long exposure times. sCMOS image sensors employ parallel and thus faster readout but suffer from significantly higher dark currents. Both camera types are area scan cameras, with a comparable sensitivity (quantum efficiency). In principle, they are both capable of measuring multiexponential decays, but this requires more complicated measurement and image processing protocols. In comparison to time-correlated single photon counting (TCSPC) scanning methods, where the whole luminescence decay curve is fitted,[36] this would not be the strongest argument for area scan cameras. Nevertheless, the image acquisition rate is high, which enables the observation of dynamic processes. In terms of lifetime determination precision both cameras are comparable, as well as in regard to pixel resolution; 1280 pixel × 1024 pixel (Sensicam Sensimod) vs 1008 pixel × 1008 pixel (pco.flim). However, the Sensicam Sensimod is limited to long lifetimes >500 ns, while the pco.flim can image shorter lifetimes (0.1 ns to 100 μs) (detailed information in Table 1, Supporting Note 2, and Table S1).

O_2 Optode Calibration. To compare the sensitivity of the two camera systems, O_2 calibration curves were measured between 0 and 207 hPa pO_2 (Figure 1A). The optodes contained the O_2 sensitive indicator dye PtTFPP in combination with diamond powder as scattering agent. The resulting Stern−Volmer plot was fitted using the simplified two-site model[37,38] (Supporting Note 3). Fitting the experimental data from the different camera systems for the same sensor foil (Figure 1B) resulted in highly similar calibration curves with K_{SV1} values of 0.027 hPa^{-1} (pco.flim)

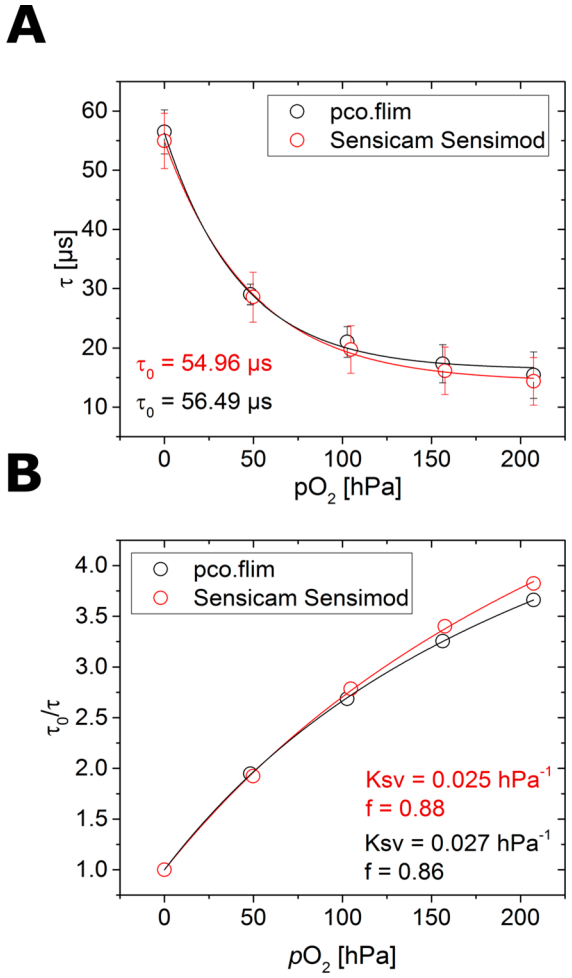

Figure 1. Comparison of O_2 calibration curves measured with TD and FD cameras. (A) Measured phosphorescence lifetimes of an O_2-optode at different O_2 levels for the FD-based pco.flim system (black) and the TD-based Sensicam Sensimod system (red). (B) Corresponding Stern−Volmer plots of the experimental data fitted with the simplified two-site model.

and 0.025 hPa^{-1} (Sensicam Sensimod) and values for the quenchable fraction (f) of 0.86 (pco.flim) and 0.88 (Sensicam Sensimod). Minor differences at higher O_2 concentrations can be explained by a lower sensitivity of the Sensicam Sensimod at lower luminescence intensity, decreasing the signal-to-noise ratio.

Comparison of Frequency-Domain and Time-Domain Camera Systems. Four different O_2-sensitive optodes based on PtTFPP as indicator dye, in combination with an antenna molecule MY,[39] and with and without diamond powder as scattering material were imaged (Figure 2A). Measurements were done on the same foils with both camera systems using the same objective and emission filter, at a constant O_2 concentration of pO_2 = 207 hPa. For the TD-camera, the addition of diamond powder remarkably reduced the obtained standard deviation of the measured phosphorescence lifetime, due to a better signal-to-noise ratio resulting from higher luminescence signal intensities. MY did neither affect the measurements with nor without diamond powder. For the FD-camera, measured lifetimes were generally higher with reduced standard deviations when MY was added, due to improved signal-to-noise ratio. The addition of diamond powder also

DOI: 10.1021/acs.analchem.8b05869
Anal. Chem. 2019, 91, 3233−3238

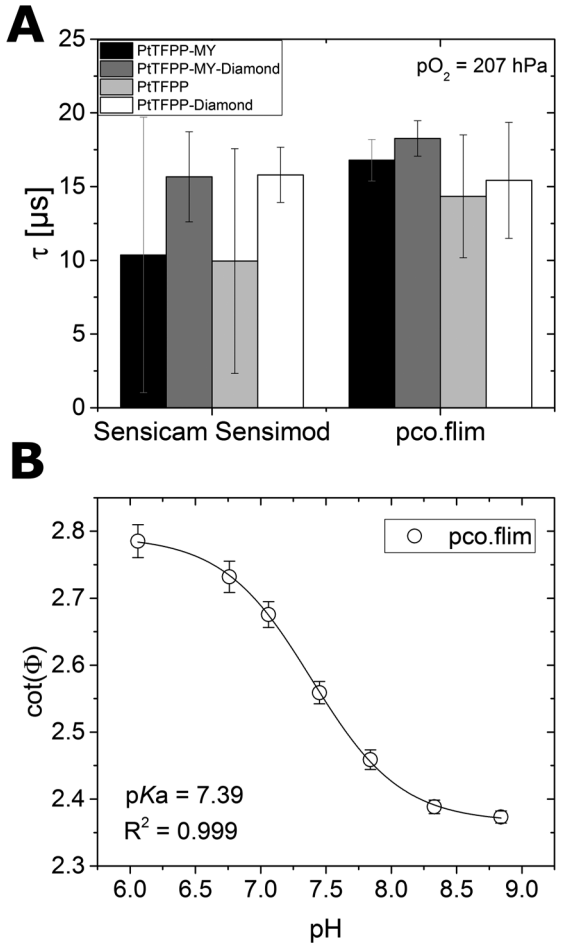

Figure 2. (A) Comparison of phosphorescence lifetimes measured with TD and FD cameras. Different planar optodes based on the O_2-sensitive indicator PtTFPP immobilized in a PS matrix are used, i.e., with MY (black), PtTFPP + MY + diamond powder (dark gray); PtTFPP by itself (light gray), and PtTFPP in combination with diamond powder (white). All images were acquired at pO_2 = 207 hPa. (B) pH imaging with the FD-based camera system via dual lifetime referencing, using OHButoxy-aza-BODIPY as a pH sensitive indicator dye and PtTPTBPF under constant O_2 concentration as a reference dye.

increased measured lifetimes; however, the effect was less pronounced than in the Sensicam Sensimod. Overall, FD-based measurements were found to be more robust, also at lower signal intensities.

Any background light (ambient light) interfered significantly with the TD-based imaging approach, while the FD-based readout was more tolerant to small amounts of background light, such as turned away desk-lamps, or nearby aquaria lights. In contrast, interference from background fluorescence, e.g. from chlorophyll or other photopigments, is less critical in TD-based measurements, where short-lived fluorescent emission can be excluded or minimized by adjusting the image acquisition windows to time intervals outside the fast decay of background fluorescence. For FD-based imaging spectrally overlapping background fluorescence affects the measured phosphorescence lifetime causing artifacts. Thus, using optodes with an optical isolation[12] when using FD-based chemical imaging of samples with background fluorescence is recommended.

Imaging pH via DLR was tested using two dyes emitting in the NIR, the pH indicator OHButoxy-aza-BODIPY[10,40] together with the O_2-sensitive PtTPTBPF.[41] The O_2 concentration was kept constant, in order to use the O_2 indicator as reference. While the pco.flim could easily resolve different pH values, the Sensicam Sensimod had too low sensitivity in the near-infrared (NIR) part of the spectrum (see also SI Figure S6). It is however shown in the literature that DLR is possible with the Sensicam Sensimod, and we recommend consulting other publications for more information.[24,42] The possibility to record DLR images makes it possible to employ not only phosphorescent but also fluorescent indicators for chemical imaging. The pco.flim system also enables the direct measurement of fluorescence lifetimes, but it requires the use of a fast modulated light source (e.g., laser diodes) instead of the LED excitation used in the present study.

Comparison of Frequency-Domain and Time-Domain Based Imaging of O_2 in a Plant Rhizosphere. For a practical comparison of the two camera systems O_2 release from roots of an aquatic plant (*Littorella uniflora*) (see Supporting Note 4) was imaged. Aquatic plants can transport O_2 from the leaves to their roots, where it is eventually released into the rhizosphere, e.g. to prevent intrusion of toxic H_2S from the sediment into the roots by oxidative processes. The roots and the surrounding sediment were brought in close contact with a planar optode. The O_2 distribution was imaged after light exposure (12 h at ~500 μmol photons m^{-2} s^{-1}) and in darkness (1 h). Both camera systems imaged the same sample and provided similar O_2 concentration images visualizing the heterogeneous chemical microenvironment in the rhizosphere (Figure 3). However, the FD-based camera system yielded slightly better image quality. Cross sections through the same root at identical locations in the O_2 images showed similar concentration profiles with maxima reaching ~43% air saturation (pco.flim) and ~44% air saturation (Sensicam Sensimod) in light and 7% air saturation (pco.flim) and 5% air saturation (Sensicam Sensimod) in darkness.

■ CONCLUSION

We investigated the potential of a rather new FD-based lifetime imaging system, namely the pco.flim, in comparison to its predecessor, the TD-based Sensicam Sensimod. To the best of our knowledge this is the first study performing phosphorescence based chemical imaging (sensing) using a FD-based imaging system. Our data show that the new pco.flim system has comparable if not better characteristics regarding chemical imaging using planar optodes, with less interference from ambient light. As the Sensicam Sensimod is no longer available due to outdated technology, the field and especially young research groups were waiting for a new system to fill the gap. We believe the pco.flim system will be able to do this and has the potential to be broadly applied in chemical imaging.

Both systems can be used as standalone devices in combination with any objective or mounted on a microscope. This enables lifetime-based chemical imaging of areas ranging from several square centimeters to square micrometers. This flexibility in spatial resolution and lifetimes (ns to μs) combined with easy handling and user-friendly data read-out makes the system attractive to various fields including life sciences,[43−45] marine biology,[46] or chemical engineering, just to name a few.

DOI: 10.1021/acs.analchem.8b05869
Anal. Chem. 2019, 91, 3233−3238

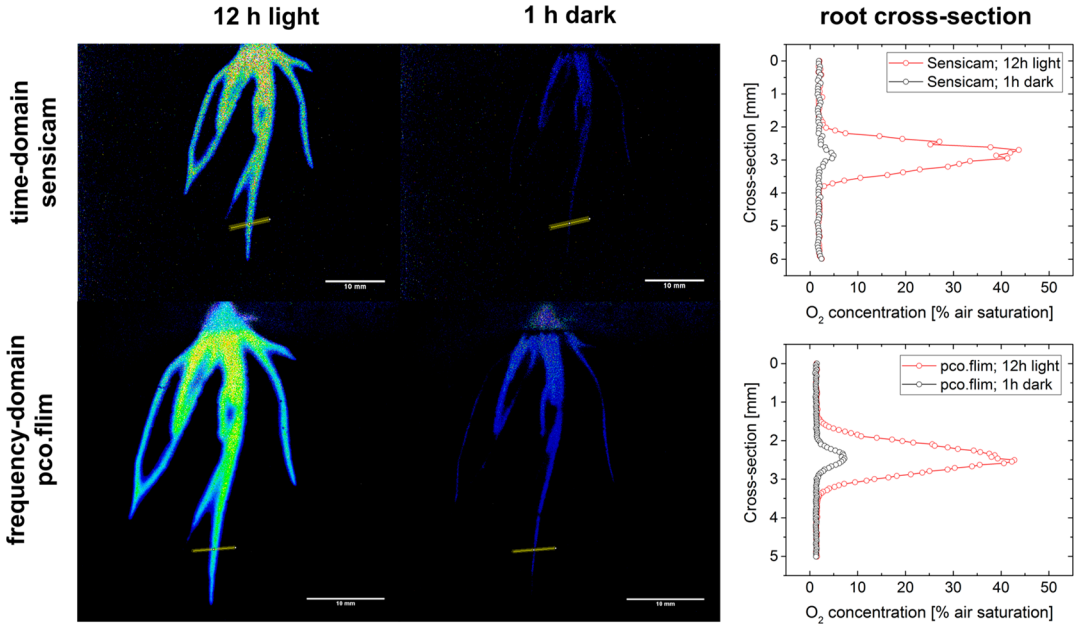

Figure 3. Comparison of FD-based and TD-based imaging of O_2 distribution in the rhizosphere of the aquatic plant *Littorella uniflora*. (top panel) Data acquired using the Sensicam Sensimod. (lower panel) Data acquired on the same plant under the same conditions using the pco.flim. (left panels) Imaging O_2 after the plant was kept for 12 h under light (~500 μmol photons m^{-2} s^{-1}). (central panels) O_2 concentration images taken after 1 h in darkness. (right panels) Cross-sectional O_2 concentration profile through the root (indicated by a yellow line in the O_2 images) after 12 h in light (red) and 1 h in darkness (black).

Obviously, the system comes with a substantial cost and has also limitations: i.e., only lifetimes up to 100 μs can be imaged and background fluorescence can be less easily overcome than in TD imaging. Nevertheless, this report shows chemical imaging has reached the frequency-domain and the system is ready to be applied widely.

■ ASSOCIATED CONTENT

Supporting Information

The Supporting Information is available free of charge on the ACS Publications website at DOI: 10.1021/acs.analchem.8b05869.

Additional theoretical information on time- and frequency-domain based image acquisition (Note 1), additional experimental details for optode preparation (Note 2), image analysis (Note 3), and plant rhizosphere sample preparation (Note 4) (PDF)

■ AUTHOR INFORMATION

Corresponding Authors

*E-mail: klaus.koren@bios.au.dk (K.K.)
*E-mail: mkuhl@bio.ku.dk (M.K.).

ORCID

Klaus Koren: 0000-0002-7537-3114
Sergey M. Borisov: 0000-0001-9318-8273

Author Contributions

§Equal contribution.

Notes

The authors declare no competing financial interest.

■ ACKNOWLEDGMENTS

We thank Sofie Lindegaard Jakobsen (University of Copenhagen) and Lars Borregaard Pedersen (Aarhus University) for technical assistance. This study was supported by a Sapere-Aude Advanced grant from the Independent Research Fund Denmark (DFF-1323-00065B; M.K.), project grants from the Independent Research Fund Denmark|Natural Sciences (DFF-8021-00308B; M.K.) & Technical and Production Sciences (DFF-8022-00301B and DFF-4184-00515B; M.K.), the Danish National Research Foundation (DNRF136), the Villum Foundation (Grant no. 00023073; M.K.), and the Poul Due Jensen Foundation (K.K.).

■ REFERENCES

(1) Schäferling, M. *Angew. Chem., Int. Ed.* **2012**, *51* (15), 3532−3554.
(2) Wang, X.-D.; Wolfbeis, O. S. *Chem. Soc. Rev.* **2014**, *43* (10), 3666−3761.
(3) Kühl, M.; Rickelt, L. F.; Thar, R. *Appl. Environ. Microbiol.* **2007**, *73* (19), 6289−6295.
(4) Quaranta, M.; Borisov, S. M.; Klimant, I. *Bioanal. Rev.* **2012**, *4* (2−4), 115−157.
(5) Brodersen, K. E.; Koren, K.; Moßhammer, M.; Ralph, P. J.; Kühl, M.; Santner, J. *Environ. Sci. Technol.* **2017**, *51* (24), 14155−14163.
(6) Zhu, Q.; Aller, R. C. *Mar. Chem.* **2013**, *157*, 49−58.
(7) Schutting, S.; Borisov, S. M.; Klimant, I. *Anal. Chem.* **2013**, *85* (6), 3271−3279.
(8) Delin, S.; Strömberg, N. *Eur. J. Soil Sci.* **2011**, *62* (2), 295−304.
(9) Santner, J.; Larsen, M.; Kreuzeder, A.; Glud, R. N. *Anal. Chim. Acta* **2015**, *878*, 9−42.
(10) Moßhammer, M.; Strobl, M.; Kühl, M.; Klimant, I.; Borisov, S. M.; Koren, K. *ACS Sensors* **2016**, *1* (6), 681−687.
(11) Borisov, S. M.; Vasylevska, A. S.; Krause, C.; Wolfbeis, O. S. *Adv. Funct. Mater.* **2006**, *16* (12), 1536−1542.
(12) Larsen, M.; Borisov, S. M.; Grunwald, B.; Klimant, I.; Glud, R. N. *Limnol. Oceanogr.: Methods* **2011**, *9*, 348−360.
(13) Koren, K.; Brodersen, K. E.; Jakobsen, S. L.; Kühl, M. *Environ. Sci. Technol.* **2015**, *49* (4), 2286.
(14) Koren, K.; Kühl, M. *Sens. Actuators, B* **2015**, *210*, 124−128.
(15) Elgetti Brodersen, K.; Koren, K.; Lichtenberg, M.; Kühl, M. *Plant, Cell Environ.* **2016**, *39* (7), 1619−1630.

DOI: 10.1021/acs.analchem.8b05869
Anal. Chem. 2019, 91, 3233−3238

(16) Meier, R. J.; Fischer, L. H.; Wolfbeis, O. S.; Schäferling, M. *Sens. Actuators, B* **2013**, *177*, 500−506.
(17) Schreml, S.; Meier, R. J.; Wolfbeis, O. S.; Landthaler, M.; Szeimies, R.-M.; Babilas, P. *Proc. Natl. Acad. Sci. U. S. A.* **2011**, *108* (6), 2432−2437.
(18) Holst, G.; Kohls, O.; Klimant, I.; König, B.; Kühl, M.; Richter, T. *Sens. Actuators, B* **1998**, *51* (1−3), 163−170.
(19) Holst, G.; Grunwald, B. *Sens. Actuators, B* **2001**, *74* (1−3), 78−90.
(20) Glud, R.; Ramsing, N.; Gundersen, J. K.; Klimant, I. *Mar. Ecol.: Prog. Ser.* **1996**, *140*, 217−226.
(21) Glud, R. N.; Tengberg, A.; Kühl, M.; Hall, P. O. J.; Klimant, I. *Limnol. Oceanogr.* **2001**, *46* (8), 2073−2080.
(22) Murniati, E.; Gross, D.; Herlina, H.; Hancke, K.; Glud, R. N.; Lorke, A. *Limnol. Oceanogr.: Methods* **2016**, *14* (8), 506−517.
(23) Schreml, S.; Meier, R. J.; Wolfbeis, O. S.; Maisch, T.; Szeimies, R.-M.; Landthaler, M.; Regensburger, J.; Santarelli, F.; Klimant, I.; Babilas, P. *Exp. Dermatol.* **2011**, *20* (7), 550−554.
(24) Grengg, C.; Müller, B.; Staudinger, C.; Mittermayr, F.; Breininger, J.; Ungerböck, B.; Borisov, S. M.; Mayr, T.; Dietzel, M. *Cem. Concr. Res.* **2019**, *116*, 231−237.
(25) Kühl, M.; Behrendt, L.; Trampe, E.; Qvortrup, K.; Schreiber, U.; Borisov, S. M.; Klimant, I.; Larkum, A. W. D. *Front. Microbiol.* **2012**, *3* (November), 402.
(26) Koop-Jakobsen, K.; Wenzhöfer, F. *Estuaries Coasts* **2015**, *38* (3), 951−963.
(27) Hancke, K.; Sorell, B. K.; Lund-Hansen, L.; Larsen, M.; Hancke, T.; Glud, R. N. *Limnol. Oceanogr.* **2014**, *59* (5), 1599−1611.
(28) Glud, R. N.; Grossart, H.-P.; Larsen, M.; Tang, K. W.; Arendt, K. E.; Rysgaard, S.; Thamdrup, B.; Gissel Nielsen, T. *Limnol. Oceanogr.* **2015**, *60* (6), 2026−2036.
(29) Larsen, M.; Santner, J.; Oburger, E.; Wenzel, W. W.; Glud, R. N. *Plant Soil* **2015**, *390*, 279.
(30) Chen, H.; Holst, G.; Gratton, E. *Microsc. Res. Tech.* **2015**, *78* (12), 1075−1081.
(31) Huber, C.; Klimant, I.; Krause, C.; Wolfbeis, O. S. *Anal. Chem.* **2001**, *73* (9), 2097−2103.
(32) Kühl, M.; Holst, G.; Larkum, A. W. D.; Ralph, P. J. *J. Phycol.* **2008**, *44* (3), 541−550.
(33) Stich, M. I. J.; Fischer, L. H.; Wolfbeis, O. S. *Chem. Soc. Rev.* **2010**, *39* (8), 3102.
(34) Klimant, I.; Huber, C.; Liebsch, G.; Neurauter, G.; Stangelmayer, A.; Wolfbeis, O. S. Dual Lifetime Referencing (DLR)−a New Scheme for Converting Fluorescence Intensity into a Frequency-Domain or Time-Domain Information. In *Fluorescence Spectroscopy*; Valeur, B., Brochon, J. C., Eds.; Springer: Berlin, 2001; pp 257−274.
(35) Franke, R.; Holst, G. A. *Proc. SPIE* **2015**, 93281K.
(36) Duncan, R. R.; et al. *J. Microsc.* **2004**, *215*, 1−12.
(37) Carraway, E. R.; Demas, J. N.; DeGraff, B. A.; Bacon, J. R. *Anal. Chem.* **1991**, *63* (4), 337−342.
(38) Klimant, I.; Ruckruh, F.; Liebsch, G.; Stangelmayer, A.; Wolfbeis, O. S. *Microchim. Acta* **1999**, *131*, 35−46.
(39) Mayr, T.; Borisov, S. M.; Abel, T.; Enko, B.; Waich, K.; Mistlberger, G.; Klimant, I. *Anal. Chem.* **2009**, *81* (15), 6541.
(40) Strobl, M.; Rappitsch, T.; Borisov, S. M.; Mayr, T.; Klimant, I. *Analyst* **2015**, *140* (21), 7150−7153.
(41) Quaranta, M.; Murkovic, M.; Klimant, I. *Analyst* **2013**, *138*, 6243−6245.
(42) Liebsch, G.; Klimant, I.; Krause, C.; Wolfbeis, O. S. *Anal. Chem.* **2001**, *73* (17), 4354−4363.
(43) Okkelman, I. A.; Foley, T.; Papkovsky, D. B.; Dmitriev, R. I. Multi-Parametric Imaging of Hypoxia and Cell Cycle in Intestinal Organoid Culture. In *Advances in Experimental Medicine and Biology*; Springer, Cham, 2017; Vol. *1035*, pp 85−103.
(44) Dmitriev, R. I.; Zhdanov, A. V.; Nolan, Y. M.; Papkovsky, D. B. *Biomaterials* **2013**, *34* (37), 9307−9317.
(45) Dmitriev, R. I.; Borisov, S. M.; Düssmann, H.; Sun, S.; Müller, B. J.; Prehn, J.; Baklaushev, V. P.; Klimant, I.; Papkovsky, D. B. *ACS Nano* **2015**, *9* (5), 5275−5288.
(46) Glud, R. N.; Wenzhöfer, F.; Tengberg, A.; Middelboe, M.; Oguri, K.; Kitazato, H. *Deep Sea Res., Part I* **2005**, *52* (10), 1974−1987.

DOI: 10.1021/acs.analchem.8b05869
Anal. Chem. 2019, 91, 3233−3238